Injection site fibroblasts acquire antigen-presenting cell properties and modulate mRNA-LNP immune responses

Azadeh Bahadoran, Mona Motwani, Ana Kume, Alessia Venturelli, Sriganesh Srihari, Mahtab Dastpak, Zon Weng Lai, Joseph McLaughlin, Robert Jordan Ontiveros, Omkar Chaudhary, Robert Amezquita, Hillary Danz, Frank DeRosa, Sudha Chivukula

Supplementary Information

Supplementary Fig. 1 Heatmap of immune pathway associated gene expression following mRNA administration

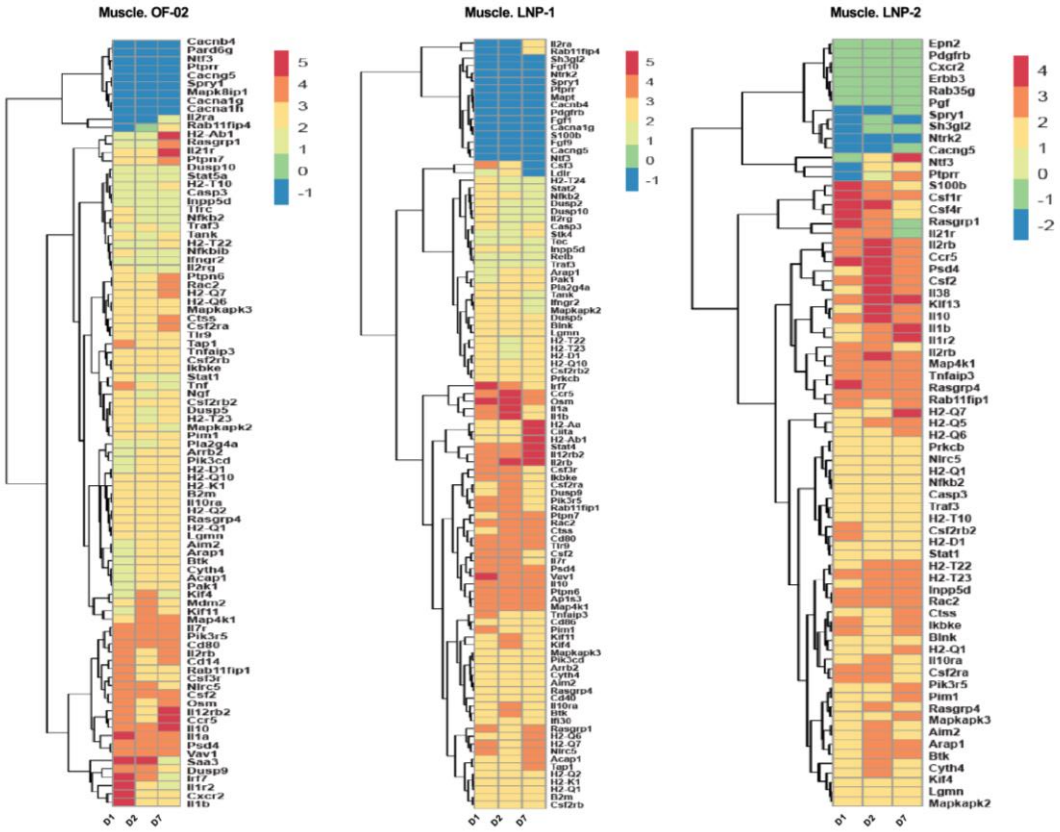

Expression heatmap of genes that map to immune pathways across the three mRNA-LNP treatments at D1, D2, and D7 at site of injection (muscle).

Commented [ND1]: More info needed in legend. What cells were analyzed?

Commented [AB2R1]: These data are from Muscle which is site of injection

Supplementary Fig. 2 Serum HAI Titers After mRNA-LNP Immunization

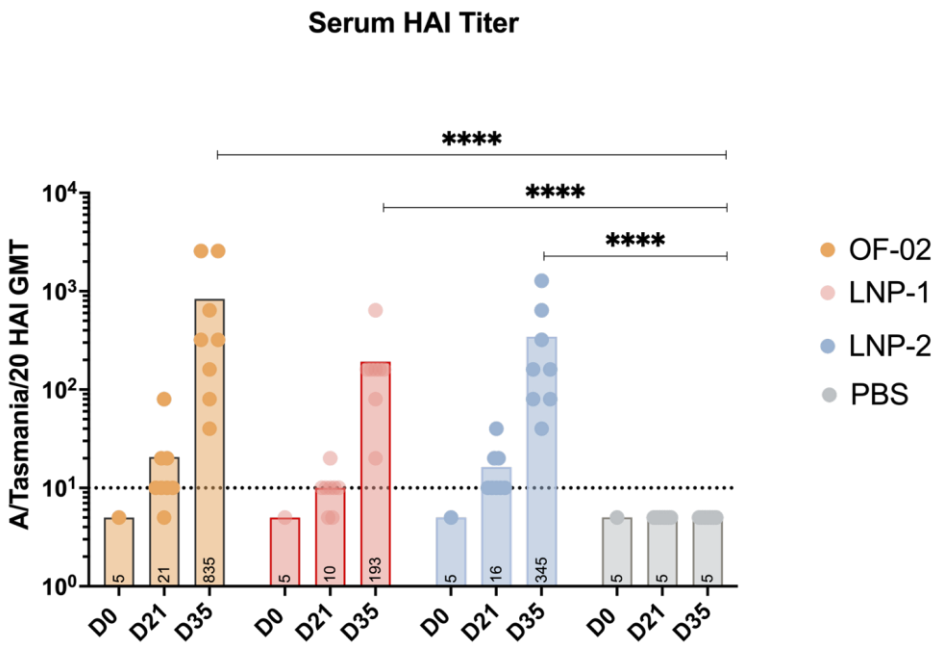

Serum hemagglutination inhibition (HAI) geometric mean titers (GMT) against A/Tasmania/20 measured at D0, D21, and D35 following immunization with different LNPs, or PBS. The dashed line denotes the assay lower limit of detection. Statistical significance is indicated as **** ($p <$ 0.0001).

Supplementary Fig. 3 Flow Cytometry Gating strategy for immune and non-immune cell populations in muscle in vivo

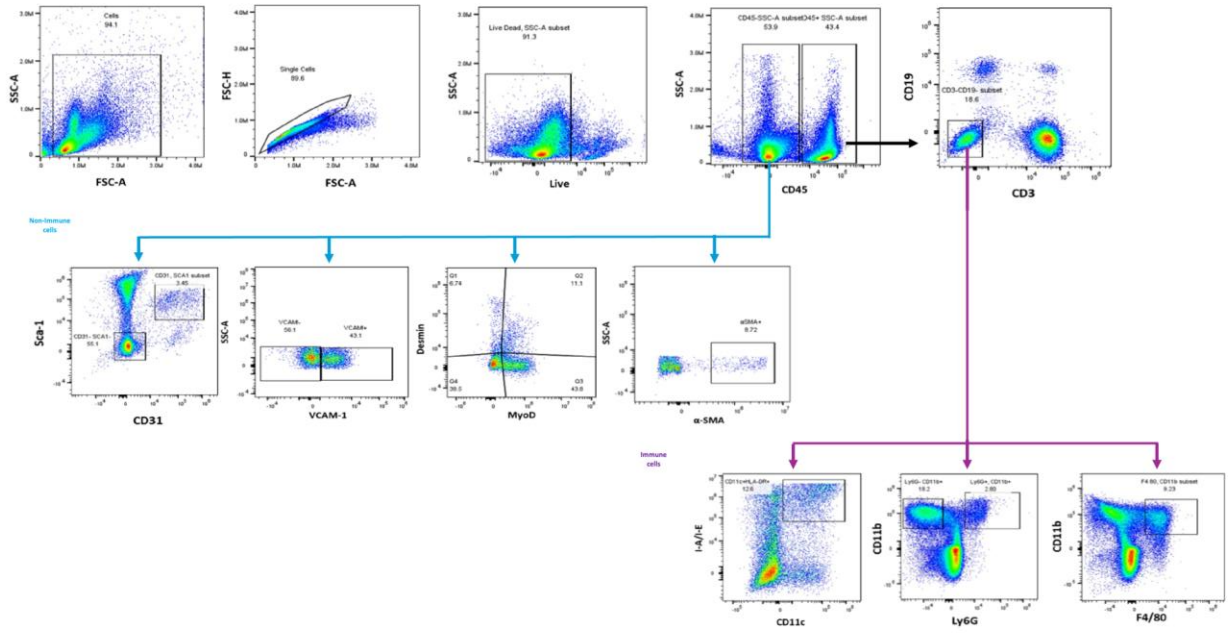

Cells were sequentially gated for singlets, live cells, and CD45 expressions to distinguish immune ($CD45^{+}$) and non-immune ($CD45^{-}$) compartments. Non-immune subsets were further defined based on CD31, Sca-1, VCAM-1, MyoD, Desmin and α-SMA expression, while immune cell populations were identified using CD11c, CD11b, Ly6G, and F4/80 markers.

Supplementary Fig. 4 Mouse perturbed-state fibroblast single-cell transcriptomic atlas interrogations

Mouse perturbed-state fibroblast single-cell transcriptomic atlas interrogations. (**A**) Re-constructed UMAP plot of mouse perturbed single-cell fibroblast dataset colored by cluster and labeled following the defining gene markers. (**B**) Dot plot of key selected gene markers across clusters depicting average expression fold change as a color gradient and dot size as the proportion of cells expressing the respective marker gene. (**C**) APC-like gene module score distributions per cluster. (**D**) Proportions of APC-high cells within each cluster (top) and proportion of APC-high cells across all clusters (bottom). (**E**) UMAP projections colored by Hallmark IFN-α (left) and IFN-γ (right) gene sets module scores across all cells. (**F**) Violin-boxplots of Hallmark IFN-α (left) and IFN-γ (right) gene set module score distributions in APC-high (red) and APC-low (grey) cell populations. **G**) Hallmark gene set pathway enrichment analysis using the APC-high-specific upregulated significant genes as the input list. The x-axis represents -log10 p-adj quantifying the statistical significance of pathway enrichment. (**H**) Dot plot depicting Gene Set Enrichment Analysis (GSEA) results using the MSigDB Hallmark gene set collection across 3 LNP formulations at days 1, 2, and 7 post-injection. Dot size represents statistical significance ($-\log_{10}$ adjusted p-value), and color intensity represents the Normalized Enrichment Score (NES), with darker red indicating stronger positive enrichment.

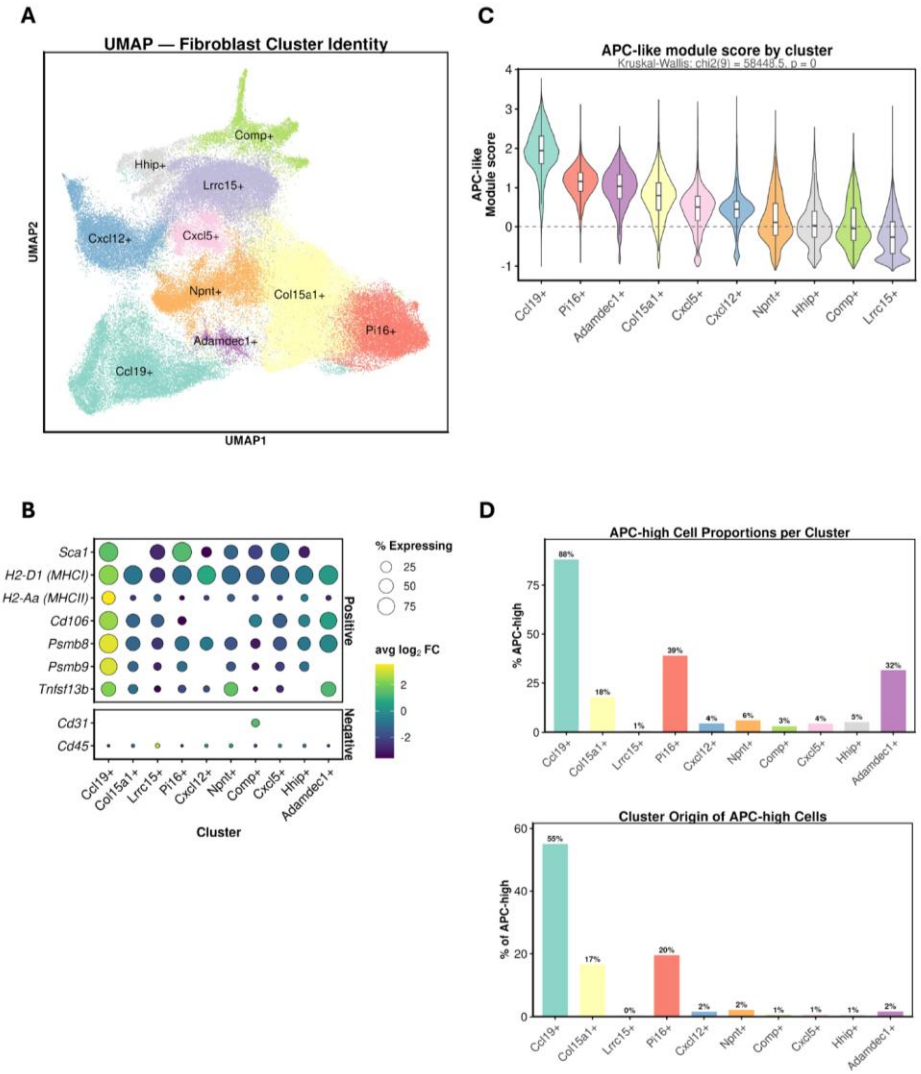
A
UMAP — Fibroblast Cluster Identity
Comp+
Hhip+
Lrrc15+
Cxcl12+
Cxcl5+
Npnt+
Col15a1+
Adamdec1+
Pi16+
Ccl19+
UMAP2
UMAP1
C
APC-like module score by cluster
Kruskal-Wallis: chi2(9) = 58448.5, p = 0
APC-like Module score
Ccl19+
Pi16+
Adamdec1+
Col15a1+
Cxcl5+
Cxcl12+
Npnt+
Hhip+
Comp+
Lrrc15+
B
Sca1
H2-D1 (MHCI)
H2-Aa (MHCII)
Cd106
Psmb8
Psmb9
Tnfsf13b
Cd31
Cd45
Positive
Negative
% Expressing
25
50
75
avg log2 FC
2
0
-2
Cluster
D
APC-high Cell Proportions per Cluster
% APC-high
88%
18%
1%
39%
4%
6%
3%
4%
5%
32%
Cluster Origin of APC-high Cells
% of APC-high
55%
17%
0%
20%
2%
2%
1%
1%
1%
2%

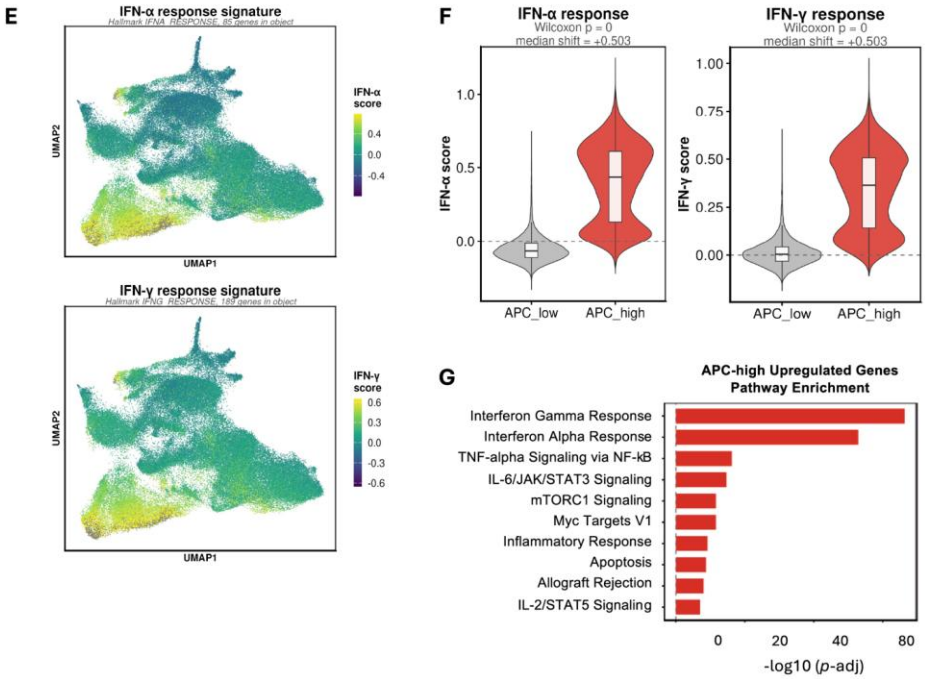
E
IFN-α response signature
Hallmark IFNA_RESPONSE, 85 genes in object
UMAP2
UMAP1
IFN-α score
0.4
0.0
-0.4
IFN-γ response signature
Hallmark IFNG_RESPONSE, 189 genes in object
UMAP2
UMAP1
IFN-γ score
0.6
0.3
0.0
-0.3
-0.6
F
IFN-α response
Wilcoxon p = 0
median shift = +0.503
IFN-α score
1.0
0.5
0.0
APC_low
APC_high
IFN-γ response
Wilcoxon p = 0
median shift = +0.503
IFN-γ score
1.00
0.75
0.50
0.25
0.00
APC_low
APC_high
G
APC-high Upregulated Genes
Pathway Enrichment
Interferon Gamma Response
Interferon Alpha Response
TNF-alpha Signaling via NF-kB
IL-6/JAK/STAT3 Signaling
mTORC1 Signaling
Myc Targets V1
Inflammatory Response
Apoptosis
Allograft Rejection
IL-2/STAT5 Signaling
0
20
40
80
-log10 (p-adj)

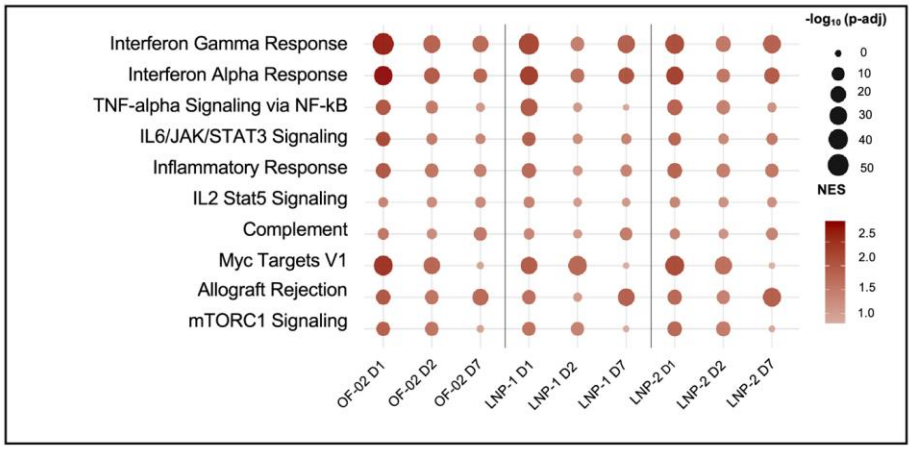
H
Pathway enrichment in CD45-negative cells
Interferon Gamma Response
Interferon Alpha Response
TNF-alpha Signaling via NF-kB
IL6/JAK/STAT3 Signaling
Inflammatory Response
IL2 Stat5 Signaling
Complement
Myc Targets V1
Allograft Rejection
mTORC1 Signaling
OF-02 D1
OF-02 D2
OF-02 D7
LNP-1 D1
LNP-1 D2
LNP-1 D7
LNP-2 D1
LNP-2 D2
LNP-2 D7
-log10 (p-adj)
0
10
20
30
40
50
NES
2.5
2.0
1.5
1.0

Supplementary Fig. 5. Immune cell trafficking profiles following mRNA-LNP administration

(**A-C**) Flow cytometric quantification of immune cell populations following IM administration of 0.4µg mRNA-LNP formulations. Fold change relative to baseline (log2 scale) is shown for (**A**) monocytes, (**B**) macrophages, and (**C**) dendritic cells at D1, D2 and D7 post-injections across different LNP formulations and PBS control. Data are presented as box-and-whisker plots. Statistical analysis was performed using two-way ANOVA followed by multiple comparisons between PBS and individual LNP formulations at each time point. Significance levels are defined as $P < 0.05$ (*), $P < 0.01$ (**), $P < 0.001$ (***), and $P < 0.0001$ (***).

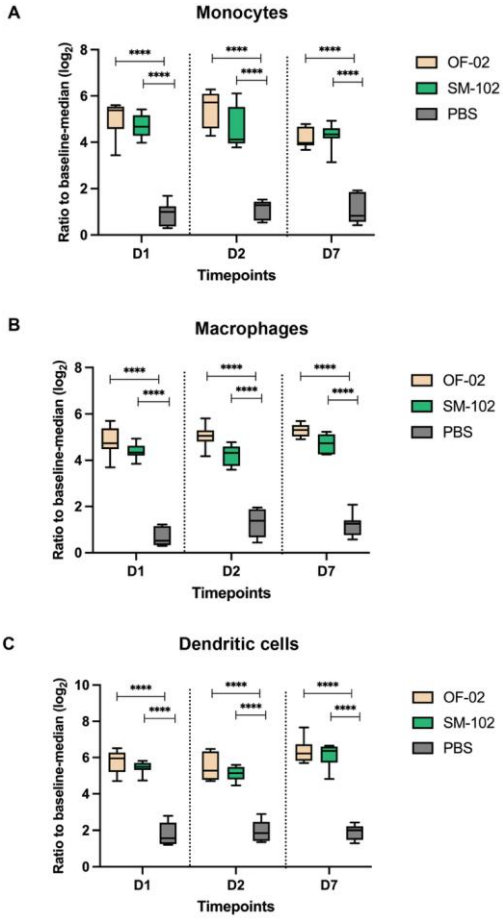

Supplementary Fig. 6 Flow cytometry gating strategy for fibroblast cells transfected with mRNA-LNP

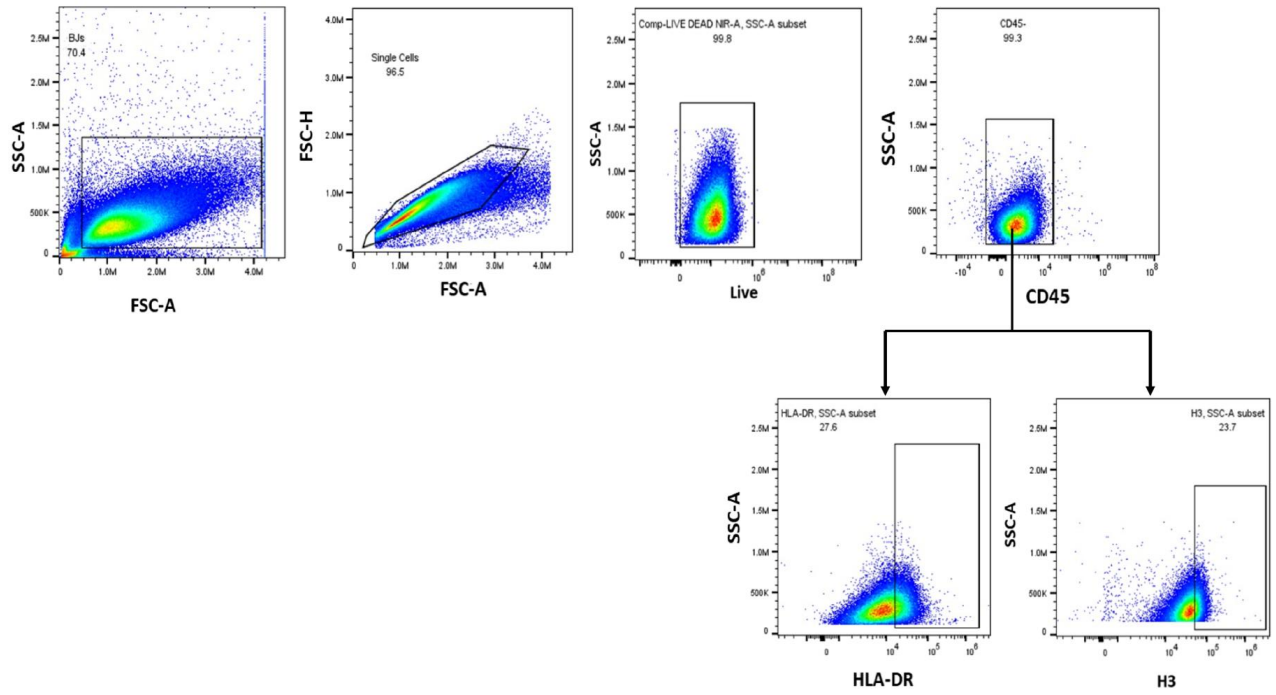

Fibroblasts (BJ cells or MEFs) were transfected with mRNA-LNP for 24 h. Events acquired by flow cytometry were gated based on FSC-A and SSC-A, followed by singlet and live cell gating. The percentage of H3-positive cells and MHC class II expression were quantified.

Supplementary Fig. 7 Flow cytometry gating strategy to analyze PBMCs co-cultured with mRNA-LNP–transfected fibroblasts

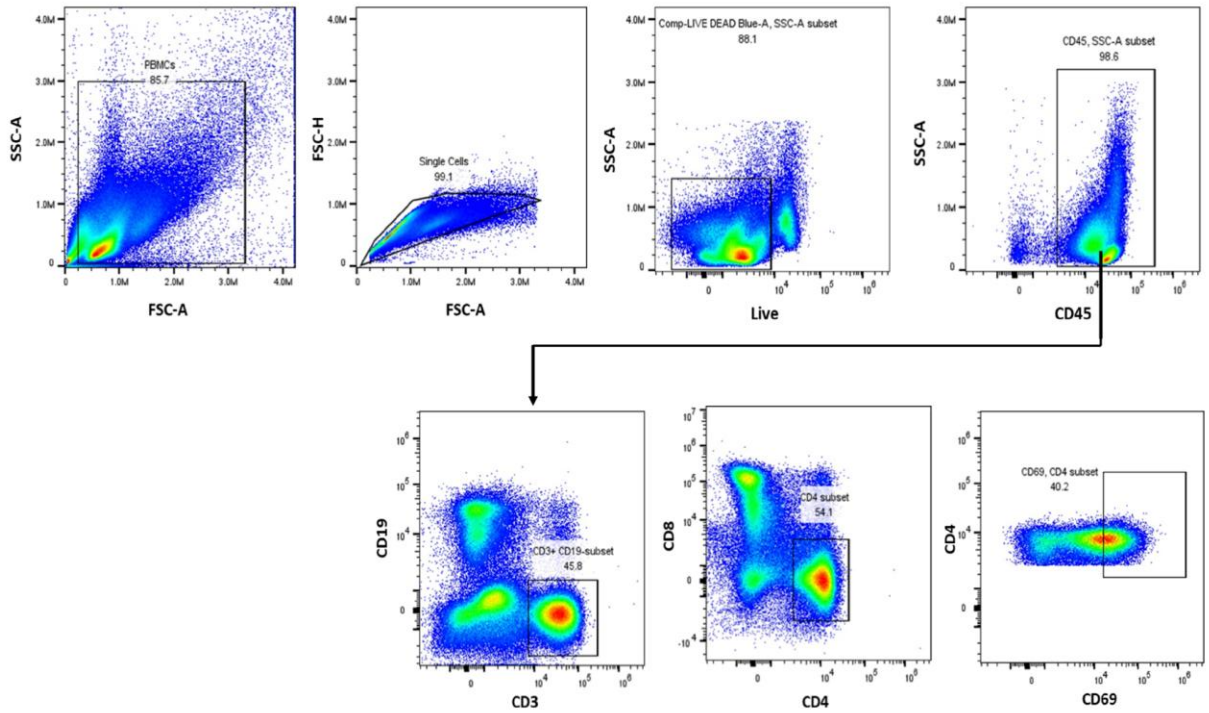

PBMCs were sequentially gated based on FSC-A/SSC-A, singlets, live cells, and CD45$^+$ events. T cells were identified as CD3$^+$ cells, with CD4$^+$ and CD8$^+$ subsets further defined. CD69 expression was assessed on CD4$^+$ T cells as a measure of activation.

Supplementary Fig. 8 Immunopeptidomics profiling of H3 antigen bound MHC-II complexes

(**A**) Total of 1,807 mouse peptides were quantified (blue) and 12 H3 immunopeptides (red) were quantified across all samples. (**B**) Unsupervised clustering of 1,807 MHC class II associated immunopeptide LC-MS intensities using Manhattan distance measure using log2-transformed peptide intensities. (**C**) Volcano plots comparing quantifiable peptides between SM-102 and LNP1 transfected cells. Data represent mean ± SEM from three independent experiments.

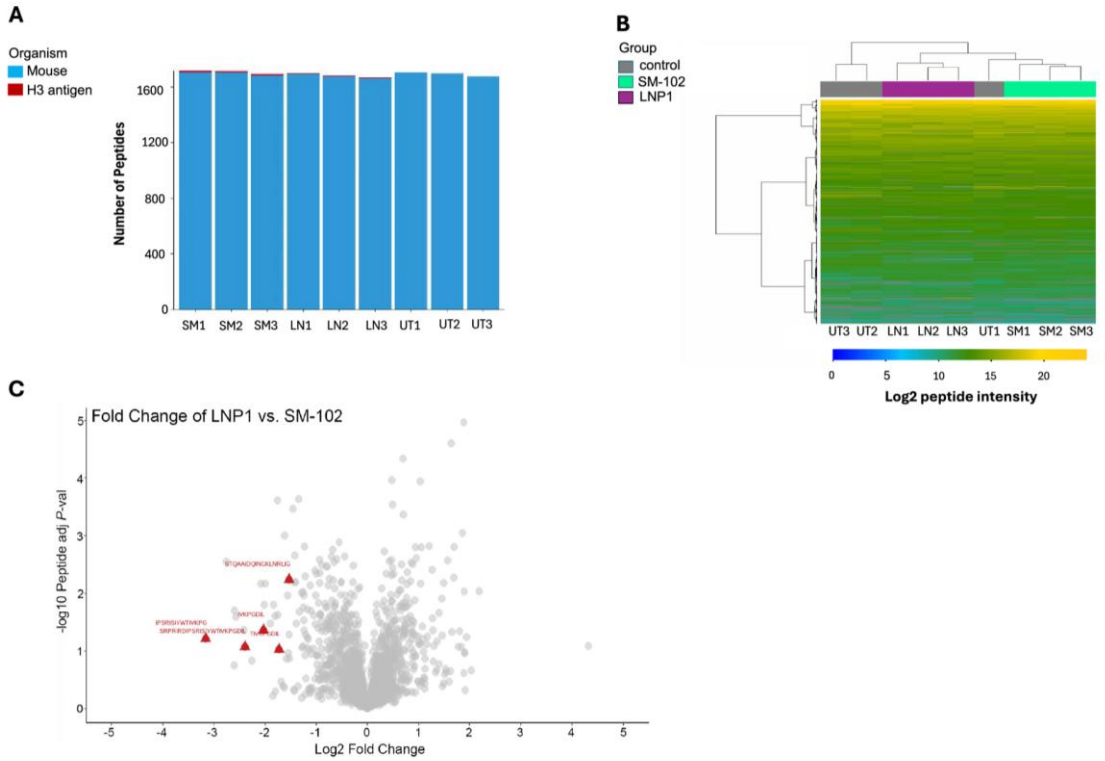

Supplementary Table 1. Characteristics of mRNA-LNPs used in the study

LNP	mRNA	Size	PDI	Encapsulation	PEG:Cat:Cholest:help
LNP-1 batch 1	H3	88	0.102	88	1.5:40:28.5:30
LNP-1 batch 2	H3	89	0.13	90	1.5:40:28.5:30
LNP-2 batch 1	H3	95	0.1	78	1.5:40:28.5:30
LNP-2 batch 2	H3	87	0.119	86	1.5:40:28.5:30
OF-02	H3	113	0.069	94	1.5:40:28.5:30
LNP-1/HL	H3	107	0.103	93	1.5:50:38.5:10
LNP-2/HL	H3	139	0.06	85	1.5:50:38.5:10
SM-102	H3	111	0.143	93	1.5:50:38.5:10
ALC-315	H3	75	0.124	97	1.5:47.5:40.7:10

Size, polydispersity index (PDI), encapsulation efficiency, and lipid composition are shown for each formulation. Batch 1 formulations were used for the data presented in Figures 1–3, whereas batch 2 formulations were used for subsequent in vivo studies and in vitro experiments.